Earth and Planetary Science
https://journals.nasspublishing.com/index.php/eps

REVIEW

Computational Review for Fluid Flow - Heat Transfer in Stress Deformation in Porous/Fractured Media, THGMC

Eduardo Teófilo-Salvador

Division of Earth Science Engineering, Faculty of Engineering, National Autonomous University of Mexico, Mexico City 04510, Mexico

ABSTRACT

Enhanced Geothermal Systems (EGS) require identifying the mathematical formulations, mechanics, thermodynamics, hydraulics, geology and chemistry. The objective was to generate a review based on the recognition of codes, and software commonly used in coupled processes of fluid flow, heat transfer, and stress deformation. The main search criterion was that the codes and software were associated with the Hot Dry Rock (HDR). The literature describing closed-loop EGS injection-production and hydraulic fracturing was reviewed. The packages were grouped into two categories: those without guides or tutorials on mathematical formulations, and those with guides and formulations. The most important parameters required for simulations were identified. Simulative applications were investigated in case studies. Simulators have evolved over the years, improved, or been coupled with other codes to generate greater accuracy. Simulators require multiple parameters including porous/fractured media, heat flux, fluid flow, wellbore, and phase interactions. Despite scientific and technological advances, they are still based on the equations of continuity, energy, momentum, and transport. They use finite difference, finite element, finite volume, discrete methods, or fractional fractal methods, transforming them into complex nonlinear systems with coupled or hybrid solutions. Hydraulic leakage processes in the rock/fracture matrix, translational heat losses, and frictional effects of fluid flow on fractures or turbulence processes are not yet clearly understood in coupled simulators. There is no universally coupled simulator that depends on a single variable, giving rise to multi-coupled systems such as Thermo-Hydro-Geo-Mechanical-Chemical (THGMC). It is advisable to review the available information to choose the appropriate computational package for HDR-based EGS studies.

Keywords: Coupled Systems; Nonlinear Systems; Complex Systems; Numerical Simulations

*CORRESPONDING AUTHOR:
Eduardo Teófilo-Salvador, Division of Earth Science Engineering, Faculty of Engineering, National Autonomous University of Mexico, Mexico City 04510, Mexico; Email: mca.ts.eduardo2015@gmail.com

ARTICLE INFO
Received: 2 February 2025 | Revised: 27 March 2025 | Accepted: 30 March 2025 | Published Online: 6 April 2025
DOI: https://doi.org/10.36956/eps.v4i1.2089

CITATION
Teófilo-Salvador, E., 2025. Computational Review for Fluid Flow - Heat Transfer in Stress Deformation in Porous/Fractured Media, THGMC. Earth and Planetary Science. 4(1): 89–108. DOI: https://doi.org/10.36956/eps.v4i1.2089

1. Introduction

Currently, nuclear waste disposal, enhanced oil and gas recovery, CO_2 storage, groundwater extraction and recharge water injection, and geothermal energy extraction in geological media are processes that can occur under multiphase flow conditions [1]. These are affected by the interaction of thermal, hydraulic, geological, mechanical, and chemical processes, and occur simultaneously. This has led to the development of coupled systems according to the governing equations, and linear and nonlinear constitutive relations.

In a porous/fractured underground medium, the flow is considered laminar to apply Darcy's equation, as a relationship between flow rate and hydraulic pressure gradient, the latter associated with hydraulic conductivity. Which is a function of the material properties (matrix permeability, or fracture transmissibility), and the fluid properties (viscosity), but which changes with temperature.

However, for forced fluid flow through fractures the Reynolds number is already important, giving rise to non-laminar regimes with turbulent tendencies, this promotes friction losses which are transformed into local heat sources. Additionally, the diffusive and advective heat transport mechanisms from the interior of the Earth to more superficial layers, thus the relationship between thermal conductivity and temperature, being a non-linear process associated with lithology.

The interaction of these mechanisms is of relevance in geosciences, and especially for Enhanced Geothermal Systems (EGS), which involve mechanical analysis of the Hot Dry Rock reservoir (HDR). Injection well stability, producer well sensitivity, as well as the number and spacing of wells for optimal heat extraction, flow paths, steady or pressurized circulation modes, long-term thermal performance, thermal contraction of the rock, and opening of fractures as the reservoir is exploited [2]. EGS have been studied since the 1970s in Fenton Hill, New Mexico, but have become novel in recent years, due to the energy potential they can provide, according to the Massachusetts Institute of Technology, which influences the available simulators.

This geothermal system involves a forced fluid flow, of cold fluid injected into a hot fractured rock matrix, leading to perturbation modeling, by poroelastic and thermoelastic effects in the rock matrix [3]. The role of the sands introduced into the fluid during the fracturing stage, is to maintain the separation between the new fractured surfaces [4,5]. The fractured system is a heat exchange medium, between the host rock matrix and the injected fluid [6]. The dual model considers two regions: the fracture network and the HDR, while the multiple models describe primary fractures, faults, and microfractures [7].

According to Clauser [8], reactions, flow and transport through the fractal network, porosity and permeability can lead to special relationships, because to high temperatures and ionic strength of the generated solution. HDR associates heat transfer and mechanical behavior of a fraction of the reservoir. Due to hydraulic fracturing, it becomes more complex by to fluid flow within fractures, on to rock deformation and propagation, such as multiscale processes, interaction between natural and hydraulic fractures, possible leaks, in addition to the difficulty in modeling by data scarcity and high associated costs [9].

For adequate long-term simulations of an HDR system, minimal numerical solutions for hydraulic flow in conductive fractures and permeable matrix, conductive and advective thermal transport, and elastic deformation of fractures and stress disturbance are required. Chemical erosion and its deposition in fractures are also important for the long-term operation of HDR.

Since 1978, literature has presented relationships between equations relating to fluid flow and heat transfer, incorporating fracturing with fundamental equations of mass, momentum, and energy [10]. Significant progress has been made in exploring, modeling, simulating and comparing of EGS [6,7,11–19].

Comparative studies have been found on individual simulation codes, or software for hydraulic, geological, thermal, mechanical, or chemical applications, but no research has been found that allows for the identification of the mathematical formulations, that represent the associated equations. Recognizing simulators by their formulations allows for the design of structures, for generating more robust models. Lack of knowledge

of the completeness, and solution schemes can lead to biases in the use of computer packages.

Mathematical misinformation can lead to mathematical, or numerical models not being sufficiently rigorous when implementing input information. Modeling geological, hydraulic, mechanical, or thermal systems is not just a matter of clicking on the easily accessible graphical interface in simulators. The importance of this research lies in the recognition of the mathematical, and/or constitutive formulations, of some of the codes or software used in highly complex nonlinear coupled, thermo-hydro-mechanical processes.

Although computers have played an important role in recent years, beyond power and availability, the reason for coupled systems is the accumulated knowledge, and unification of principles provided by past and present research in the field of numerical simulation [20]. Current packages allow reservoir behavior to be predicted and, from this, a lifetime inferred under operating, stability, steady-state, and transient conditions. Solving the governing equations simultaneously allows, for progress in understanding highly nonlinear thermo-hydro-geo-mechanical processes, such as EGS, that are difficult to study with physical experiments.

Therefore, the objective was to generate a didactic method for recognizing codes, and software commonly used in coupled processes associated with fluid flow, heat transfer and stress deformation.

2. Materials and Methods

The conceptual model shown in **Figure 1** was proposed for an HDR EGS. A deep injection well was proposed, a high-temperature reservoir with hydraulic fractures, at a certain distance a producer well was located. The lower, lateral and upper boundaries are impermeable, and the fluid flow injection as the hydraulic source at high pressures. The following were proposed: (i) a hydraulic transition zone by contact between the fluid flow, and the rock matrix, (ii) a mechanical transition zone associated with high-pressure deformations, primary fractures and residual fractures, (iii) a thermal transition zone where the matrix-hydraulic fracture is the heat transfer medium to the fluid flow, and (iv) a chemical transition zone with particle deposition at the entrance of the producer well. It was assumed that there are no fluid flow losses between fractures, that all the fluid is mobilized in the fractures, and that temperature variations are minimal at high fluid velocities.

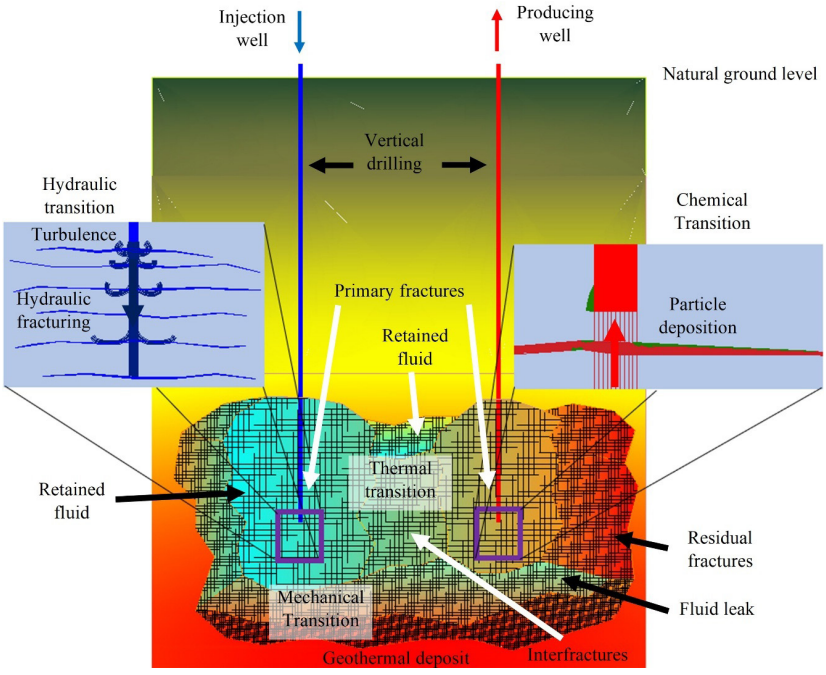

Figure 1. Conceptual Model of the Interaction of Thermal, Hydraulic, Mechanical and Chemical Processes in the EGS HDR (Own Elaboration).

This model (**Figure 1**), shows the interaction between thermal effects from the reservoir bed, fluid flow from hydraulic injection, deformation from hydraulic fracturing stresses, and high pressures. Additionally, chemical effects represent a thermo-hydro-geo-mecha-chemical (THGMC) system. Based on **Figure 1**, the formulations of commonly used codes or simulators for fluid flow interaction, heat transfer, and stress deformation processes in porous/fractured media were reviewed. **Table 1** summarizes the simulators that have been implemented, with geo-mechanical approach [2,21,21–24]. **Table 2** shows the simulators with mathematical formulations [1,3,8,20,25–38].

Consecutively were investigated applications, which associated coupled processes. Some characteristics of the simulators were identified. This allowed to generate an analysis, of how these codes or software have evolved, and how disciplines are related, from their various mathematical formulations.

Table 1. Introduction to Simulators Commonly Used in Fluid Flow, Heat Transfer, and Stress Deformation Processes: Geo-Mechanics (Own Elaboration).

SOFTWARE/CODE	DESCRIPTION
STAR [21] General-purpose geothermal reservoir simulator	Hydrothermal, natural gas, oil, for reservoir simulation with pressure, temperature transients, fractures, and rock matrix. Input: Formation, grain density, porosity, heat capacity, thermal conductivity, modulus of elasticity, horizontal and vertical permeability.
GEOCRACK [2,22]	Coupled to rock formation, fluid flow, heat transfer, steady-state, periodic pressurization, energy availability behaviors, with finite element solution. Input: Reservoir geometry: thickness, x and y spacing. Mechanical: stresses in x and y, field permeability, and closure stresses. Hydraulic: fluid roughness factor, viscosity, density, heat capacity, conductivity, and fluidic coefficient. Thermal: rock temperature, density, heat capacity, conductivity, thermal expansion, modulus of elasticity, and Poisson's ratio.
GEOTH3D [21,23]	It uses finite-difference microseismicity, to solve the mass-energy equation based on Darcy's law, it can describe water and heat transport, and it has been applied to well measurements, for injection and production pressures.
GEOSIM Geomechanics simulator [24]	Coupled geomechanical modeling of 3D reservoirs, three-phase for thermal reservoirs, with finite elements, and stress-strain with modules (TERASIM-THERM three-phase simulation model for thermal flow modeling, FEM3D 3D finite-element). Input: Porosity-dependent pressure, linear or nonlinear stress and strain, and temperature. Reservoir properties: formation, number of layers, depth, thickness, permeability, porosity, initial pressure, water saturation, Young's modulus, Poisson's ratio, relative permeability, initial stress, transmissibility, stress gradient, average total and effective stress.

Table 2. Simulators Commonly Used in Fluid Flow, Heat Transfer, and Stress Deformation Processes, with Some Formulation'S Formulations (Own Elaboration).

SOFTWARE/CODE	MODELS/SOLUTION OF EQUATIONS BASE
TETRAD (a group of four) [20]	$$\frac{\partial}{\partial t}\left[\phi\left(\rho_w W_c S_w + \rho_g Y_c S_g + \rho_o X_c S_o\right)\right] = -\nabla\frac{\rho_w k_w k W_c}{\mu_w}\cdot\nabla\psi_w - \nabla\frac{\rho_g k_g k Y_c}{\mu_g}\cdot\nabla\psi_g - \nabla\frac{\rho_o k_o k X_c}{\mu_o}\cdot\nabla\psi_o + q_c \quad (1)$$ $$\nabla\psi_w = \nabla\left(P - P_{cwo}\right) - M_w\rho_w g \quad (2)$$ Where q_c is the source, the potential ψ includes capillarity and gravity g, $k_{o,w,g}$ the gas or water phase permeability, k absolute permeability, P phase pressure, q the source or sink, t time, W mole fraction in the water phase, S saturation, X mole fraction in the oil phase, Y mole fraction in the gas phase, *cwo* water-oil capillarity, μ viscosity, ρ density, ϕ porosity, w water, o oil and g gas.

Table 2. *Cont.*

SOFTWARE/CODE	MODELS/SOLUTION OF EQUATIONS BASE
TOUGH2 [25] Transport Of Unsaturated Groundwater and Heat	$\frac{d}{dt}\int_{V_n} M^{\kappa} dV_n = \int_{\Gamma_n} \mathbf{F}^{\kappa}\cdot\mathbf{n}d\Gamma_n + \int_{V_n} q^{\kappa} dV_n \ , \ M^{\kappa} = \phi\sum_{\beta} S_{\beta}\rho_{\beta}X_{\beta}^{\kappa}$ (3) $M^{NK+1} = (1-\phi)\rho_R C_R T + \phi\sum_{\beta} S_{\beta}\rho_{\beta}u_{\beta}$ (4) For an arbitrary volume V_n of the flow system, Γ_n is the closed surface, M the heat accumulation as mass or energy per unit volume, κ mass components (agua, aire, H_2, solutos), $\mathbf{F}$ the mass or heat flux, q the source or sink, $\mathbf{n}$ a normal vector on the surface element $d\Gamma_n$. β is liquid, gas, NAPL, ϕ porosity, S_β the saturation phase, ρ_β = the phase density, X^{κ}_{β} the mass fraction of component κ in the β phase. For heat accumulation in a multiphase system, ρ_R is the grain density, C_R the specific heat of the rock, T the temperature, u_β the specific internal energy in the β phase. The advective mass flux is: $\mathbf{F}^{\kappa}\big\|_{adv} = \sum_{\beta} X_{\beta}^{\kappa}\mathbf{F}_{\beta}$ (5) For the individual flow phase, Darcy's law: $\mathbf{F}_{\beta} = \rho_{\beta}\mathbf{u}_{\beta} = -k\frac{k_{r\beta}\rho_{\beta}}{\mu_{\beta}}\left(\nabla P_{\beta} - \rho_{\beta}\mathbf{g}\right)$ (6) With u_β being the Darcy velocity, k the absolute permeability, $k_{r\beta}$ the relative permeability, μ_β the viscosity, P_β = $P + P_{c\beta}$, pressure P and capillary pressure $P_{c\beta}$, and g the gravitational constant. Neglecting phase change effects, gas pressure gradients for flow in the liquid phase: $\frac{\partial}{\partial t}\phi S_l\rho_l = div\left[k\frac{k_{rl}}{\mu_l}\rho_l\nabla\left(P_l + \rho_l g z\right)\right]$ (7) With z as the positive direction, neglecting variations in liquid phase density and viscosity, simplified to Richard's equation: $\frac{\partial}{\partial t}\theta = div\left[K\nabla h\right]$ (8) $\Theta = \phi S_l$ as specific volumetric moisture content, $K = kk_{rl}\rho_l g/\mu_l$ the hydraulic conductivity, and $h = z + P_l/\rho_l g$ the hydraulic head.
FRACTure [3], Flow, Rock And Coupled Temperature effects	Buoyancy superimposed on Darcy's Law behavior: $S_s\cdot\frac{dP}{dt} - \nabla\left[\frac{k}{\mu}\cdot\nabla P - \left(\rho_f - \rho_{fo}\right)\cdot g\cdot\nabla z\right] = 0$ (9) S_s specific storage coefficient, P hydraulic pressure, μ dynamic viscosity, k the permeability matrix, ρ_{fo} reference fluid density, ρ_f fluid density, and g the gravitational constant. The hydraulic regime in fracture: $T = \frac{k\cdot a_h}{\mu}$ (10) T is the fracture transmissibility, and a_h the hydraulic aperture. The turbulent hydraulic regime in fractures: $v_d = -\left(K^* = 4\cdot\frac{\sqrt{a_h}}{\sqrt{g\cdot\rho}}\cdot\log\left[\frac{3.7}{k/D_h}\right]\right)\cdot\left|\nabla P\right|^{-0.5}\cdot\nabla P$ (11) With v_d Darcy flow velocity, ∇P pressure gradient, and k/D_h being the relative roughness. Thermal transport: $\overline{\rho c_p}\cdot\frac{dT}{dt} + \left[\rho c_p\right]_f\cdot v_d\cdot\nabla T - \lambda\cdot\nabla^2 T + H = 0$ (12) Where ρc_p is the average specific heat capacity of the fluid-solid phase mixture, λ is the thermal conductivity tensor, $[\rho c_p]_f$, T is the temperature, and H is the heat resource. Rock mechanics: $\sigma_{ij} = c_{ijkl}\cdot\varepsilon_{kl}$ (13) The effective stresses σ_{ij} equal to the stiffness matrix c_{ijkl} and the stress component ε_{kl}.
FRACSIM-3D [26] Three-dimensional simulation of flow analysis	The radius of a random chosen fracture: $r_\alpha = \left[(1-\alpha)r_{\min}^{-D} + \alpha r_{\max}^{-D}\right]^{-1/D}$ (14) Where α is random from 0 to 1, r_{max} and r_{min} radius limits, D is the fractal dimension, with fracture opening: $a_0 = \beta r_l$ (15) With r_l being the fracture radius, and β being the proportionality constant. Mohr-Coulomb criterion:

Table 2. *Cont.*

SOFTWARE/CODE	MODELS/SOLUTION OF EQUATIONS BASE
	$$\tau > (\sigma_n - p)\tan\left[\phi_{basic} + \left(\phi_{dil}^{eff} = \frac{\phi_{dil}}{1+9\left(\frac{\sigma_n - p}{\sigma_{nref}}\right)}\right)\right] \quad (16)$$ Where τ is shear stress, σ_n total normal stress, p fluid pressure in the fracture, ϕ_{basic} basic friction angle of rock material from 30° to 40°, ϕ^{eff}_{dil} dilated effective shear stress angle, σ_{nref} effective normal stress, and shear dilation angle ϕ_{dil}. The shear displacement is: $$U = \frac{\tau - (\sigma_n - p)\tan\left(\phi_{basic} + \phi_{dil}^{eff}\right)}{\left(K_s = \gamma\frac{G}{R}\right)} \quad (17)$$ With K_s fracture shear stiffness, γ geometric parameter, G shear modulus and R fracture radius. For the flow rate: $$Q = \frac{ia^3\Delta P}{12\mu L} \quad (18)$$ With L as the block length, ΔP pressure fraction, a fracture opening, μ the viscosity, and i the intersected fracture length.
TOUGH-FLAC3D [1] Fast Lagrangian Analysis of Continua in 3 Dimensions	The total mass balance in component: $$\frac{\partial}{\partial t}M^\kappa - Q^\kappa = -\nabla\cdot\left(\mathbf{q}_l^\kappa + \mathbf{q}_g^\kappa\right),\ M^\kappa = \phi S_l\rho_l X_l^\kappa + \phi S_g\rho_g X_g^\kappa \quad (19)$$ $$\mathbf{q}_\psi^\kappa = -\rho_\psi X_\psi^\kappa\frac{\mathbf{k}k_{r\psi}}{\mu_\psi}\left(\nabla P_\psi - \rho_\psi g\nabla z\right) + \mathbf{i}_\psi^\kappa,\ \mathbf{i}_\psi^\kappa = -\rho_\psi D_v\mathbf{I}\nabla X_\psi^\kappa \quad (20)$$ The conservation of assembled energy is: $$\frac{\partial}{\partial t}\left(\phi S_l\rho_l e_l + \phi S_g\rho_g e_g + (1-\phi)\rho_s C_s T\right) - Q^h = -\nabla\cdot\left(\mathbf{q}^h\right),\ \mathbf{q}^h = \sum_\psi\sum_\kappa h_\psi^\kappa\mathbf{q}_\psi^\kappa + \mathbf{i}_m^h,\ \mathbf{i}_m^h = -\lambda_m\mathbf{I}\nabla T \quad (21)$$ To FLAC3D: $$\nabla\cdot\boldsymbol{\acute{o}} + \rho_m\mathbf{g} = \rho_m\frac{d\mathbf{v}}{dt},\ \dot{\varepsilon} = \frac{1}{2}\left(\nabla\mathbf{v} + (\nabla\mathbf{v})^{\mathrm{tr}}\right) \quad (22)$$ Coupling: $$\frac{\partial}{\partial t}M^\kappa + M^\kappa\alpha\frac{\partial\varepsilon_v}{\partial t} - Q^\kappa = -\nabla\cdot\left(\mathbf{q}_{rl}^\kappa + \mathbf{q}_{rg}^\kappa\right) \quad (23)$$ Where κ (a for air, w for water, k for CO_2), M for mass per unit volume of component κ, ϕ for porosity, S_ψ and ρ_ψ are saturation and density of phase ψ (g gas, l liquid), X_ψ^κ is the mass fraction of component κ in fluid phase ψ, the mass flow of each component as q, diffusive flux i, D_v effective molar diffusion coefficient, e the internal energies of each phase, C_s specific heat, $\mathbf{q}^h$ energy flux density, Q^h thermal heat source, h_ψ^κ is enthalpy of component κ in fluid phase ψ, λ_m apparent macroscopic thermal conductivity, $\dot{\varepsilon}$ is the infinitesimal strain-rate tensor, α is Biot´s effective stress parameter, P pore pressure, ε_v volumetric strain, and subscript r on the flux terms indicates mass flux relative to the solid phase.
SHEMAT Simulator for HEat and MAss Transport [8]	Underground flow: $$\rho_f\left(\alpha + \phi\beta\right)\frac{\partial P}{\partial t} = \nabla\left[\frac{\rho_f k}{\mu}\left(\nabla P + \rho_f g\nabla z\right)\right] + W_s\rho^* \quad (24)$$ Where ρ_f is the fluid density, ρ_0 is the reference density, ϕ porosity, P is the pressure, k is the permeability, α is the rock compressibility, β is the fluid compressibility, W is the source or sink, W_s specific source strength, and z is the coordinate. Heat transport: $$\int_V\frac{\partial Q}{\partial t}dV = \int_V\frac{\partial}{\partial t}\left(\rho_c T\right)dV = \int_F\left(\lambda\nabla T - \rho_f c_f T\mathbf{v}\right)\mathbf{n}dF + \int_V HdV \quad (25)$$ Where the left side is the change in heat content as a function of time for a given volume, and the right side integrates for diffusion, advection, and heat production, $\mathbf{n}$ is the unit vector associated with the surface F, T temperature.

Table 2. *Cont.*

SOFTWARE/CODE	MODELS/SOLUTION OF EQUATIONS BASE
IPARS (Integrated Parallel Accurate Reservoir Simulator) – JAS3D [27,28]	Material balance component: $$V_b \frac{\partial N_i}{\partial t} - V_b \overset{\rho}{\nabla} \cdot \sum_{j=1}^{n_p} \xi_j \frac{kk_{rj}}{\mu_j} x_{ij} \left(\nabla P_j - \gamma_j \nabla D \right) - q_i = 0 \quad , \quad i = 1,2,..,n_c \tag{26}$$ Phase equilibrium relationship: $$f_i = \left[f_i^j = \ln\left(\pi x_{ij} \phi_{ij} \right) \right] - f_i^r = 0 \, , \; i = 1,2,L,n_c \, , \; j = 1,2,L,n_p \, , \text{ for } \left(n_p - 1 \right) n_c \tag{27}$$ Volume and capillarity: $$V_b \sum_{i=1}^{n_c} N_i \sum_{j=1}^{n_p} L_j \bar{v}_j - V_p = 0 \tag{28}$$ Molar energy balance: $$\frac{\partial u}{\partial t} + \overset{\rho}{\nabla} \cdot \le \sum_{j=1}^{n_p} \xi_j \lambda_j h_j \left(\nabla P_j - \gamma_j \nabla D \right) - \overset{\rho}{\nabla} \cdot \left(\lambda_T \nabla T \right) - q_H + q_L = 0 \tag{29}$$ D is the depth, f_i residual, f_i^a fugacity of component i, h_j enthalpy, k permeability, k_{rj} relative permeability, N_i moles of component i ,n_b number of cells, n_c number of components, n_p number of phases, P_j phase pressure, q_i molar injection or production, q_H enthalpy of injection rate, q_L heat loss, T temperature, t time, V_b bulb volume, V_p pore volume, v_j molar volume, x mole fraction component, γ gravity term, ξ molar density, λ effective thermal conductivity of the rock, μ viscosity, ρ density, and ϕ porosity. Darcy´s law gives the mass velocity U of phase i: $$U_i = -\frac{Kk_{ri}}{B_i \mu_i} \cdot \left(\nabla P_i - \rho_i g \nabla D \right) \tag{30}$$ K is the absolute permeability tensor, k_{ri} the relative permeability of phase i, B_i the formation volume factor for phase i, P_i pressure, μ_i viscosity, ρ_i density, g gravity, and D depth.
MOTIF (Model of Transport in Fractured/porous media) [29]	Equations to describe thermohydroelastic: $$e_{ij} = C_{ijkl}^{-1} \left(\tau_{kl} - \tau_{kl}^o \right) + \Delta p U_{ij} + \Delta T W_{ij} \, , \; e_{ij} = \frac{1}{2} \left(\frac{\partial u_i}{\partial x_j} + \frac{\partial u_j}{\partial x_i} \right) \tag{31}$$ $$\tau_{kl} = C_{ijkl} e_{kl} - \Delta p U_{ij}^* - \Delta T W_{ij}^* + \tau_{ij}^o \, , \; U_{ij}^* = C_{ijkl} U_{ij} \, , \; W_{ij}^* = C_{ijkl} W_{ij} \tag{32}$$ Where e_{ij} is the strain tensor, u_i is the strain in the i-direction, C_{ijkl} is the elastic tensor constant, τ_{ij} is the stress tensor, $\tau^o{}_{ij}$ is the initial stress tensor, U_{ij} is the hydroelastic isothermal tensor constant, W_{ij} is the thermoelastic isothermal tensor constant, x_i is the coordinate in the x-direction, p is the fluid pressure, p_{ref} is the reference fluid pressure, $\Delta p = p - p_{ref}$, T is the temperature, and T_{ref} is the reference temperature, $\Delta T = T - T_{ref}$.
FEHM (Finite Element Heat and Mass) [30,31]	Simultaneous heat and mass transfer solution: $$R_{mi} = V_i \frac{\left[\left(\phi \left(\rho_l S_l + \rho_v S_v \right) \right)_i^{n+1} - \left(\phi \left(\rho_l S_l + \rho_v S_v \right) \right)_i^n \right]}{\Delta t} - \sum_{\substack{neighbor \\ cells}} \left(\frac{k \rho_l}{\mu_l} R_l \right)_{ij} \cdot \left(\frac{A_{ij}}{\Delta d_{ij}} \right) \cdot \left[\left(P_{lj} - P_{li} \right) - \left(\rho_l g \right)_{ij} \left(z_j - z_i \right) \right]$$ $$- \sum_{\substack{neighbor \\ cells}} \left(\frac{k \rho_v}{\mu_v} R_v \right)_{ij} \cdot \left(\frac{A_{ij}}{\Delta d_{ij}} \right) \cdot \left[\left(P_{vj} - P_{vi} \right) - \left(\rho_v g \right)_{ij} \left(z_j - z_i \right) \right] + q_{mi} \tag{33}$$ $$R_{ei} = V_i \frac{\left[\left(\left(1 - \phi \right) \rho_r u_r + \phi \left(\rho_l u_l S_l + \rho_v u_v S_v \right) \right)_i^{n+1} - \left(\left(1 - \phi \right) \rho_r u_r + \phi \left(\rho_l u_l S_l + \rho_v u_v S_v \right) \right)_i^n \right]}{\Delta t}$$ $$- \sum_{\substack{neighbor \\ cells}} \left(\frac{k \rho_l h_l}{\mu_l} R_l \right)_{ij} \cdot \left(\frac{A_{ij}}{\Delta d_{ij}} \right) \cdot \left[\left(P_{lj} - P_{li} \right) - \left(\rho_l g \right)_{ij} \left(z_j - z_i \right) \right] - \sum_{\substack{neighbor \\ cells}} \left(\frac{k \rho_v h_v}{\mu_v} R_v \right)_{ij} \cdot \left(\frac{A_{ij}}{\Delta d_{ij}} \right) \cdot \left[\left(P_{vj} - P_{vi} \right) - \left(\rho_v g \right)_{ij} \left(z_j - z_i \right) \right] \tag{34}$$ $$- \sum_{\substack{neighbor \\ cells}} K_{ij} \cdot \left(\frac{A_{ij}}{\Delta d_{ij}} \right) \cdot \left(T_j - T_i \right) + q_{ei}$$ Where ϕ is the porosity, t the time, g the gravitational constant, μ the viscosity, P the pressure, k the intrinsic permeability, u the internal energy, h the enthalpy, K the thermal conductivity, T the temperature, the subscripts l and v referred to liquid or vapor, m the mass and e the energy, and the area factor $A_{ij}/\Delta d_{ij,}$

Table 2. *Cont.*

SOFTWARE/CODE	MODELS/SOLUTION OF EQUATIONS BASE
HYDROTHERM [32]	Underground flow equation: $$\frac{\partial}{\partial t}\left[\phi\left(\rho_w S_w+\rho_s S_s\right)\right]-\nabla\cdot\frac{\mathbf{k}k_{rw}\rho_w}{\mu_w}\left[\nabla p+\rho_w g\hat{\mathbf{e}}_z\right]-\nabla\cdot\frac{\mathbf{k}k_{rs}\rho_s}{\mu_s}\left[\nabla p_g+\rho_s g\hat{\mathbf{e}}_z\right]-q_{sf}=0 \quad (35)$$ Where ϕ is the porosity, ρ is the fluid density, S_p is the water saturation, **K** is the permeability tensor of the porous medium, k_r is the relative permeability, μ is the viscosity, p is the fluid pressure, p_g fluid pressure in the gas phase, g is the gravitational constant, $\mathbf{e}_z$ is the unit vector in the z direction, q_{sf} is the flow rate intensity, and t is the time. Thermal energy transport equation: $$\frac{\partial}{\partial t}\left[\phi\left(\rho_w h_w S_w+\rho_s h_s S_s\right)+\left(1-\phi\right)\rho_r h_r\right]-\nabla\cdot K_a\mathbf{I}\nabla T+\nabla\cdot\phi\left(S_w\rho_w h_w\mathbf{v}_w+S_s\rho_s h_s\mathbf{v}_s\right)-q_{sh}=0 \quad (36)$$ Where h is the specific enthalpy of the fluid phase, h_r specific enthalpy of the porous-matrix solid phase, K_a the effective thermal conductivity, **I** the identity matrix, T the temperature, and q_{sh} the flow rate intensity of the source.
FALCON (Fracturing And Liquid Convection) [33]	Mass fluid balance: $$\frac{\partial(\varphi\rho_w)}{\partial t}+\nabla\cdot(\rho_w\mathbf{u}_\mathbf{w})-q'_w=0 \quad (37)$$ With $\mathbf{u}_w$ the flow vector, ρ_w the fluid density, and ϕ the reservoir porosity. Fluid momentum equilibrium: $$\mathbf{u}_\mathbf{w}=-\frac{k}{\mu_w}\cdot\left(\nabla p_w-\rho_w g\nabla z\right) \quad (38)$$ Where k is the intrinsic permeability of the reservoir, μ_w is the fluid viscosity, g is the acceleration of gravity, and z is the directional component. Energy balance: $$\frac{\partial[\varphi\rho_w h_w]}{\partial t}+\nabla\cdot(\rho_w h_w\mathbf{u}_\mathbf{w})+\nabla\cdot\lambda_{cw}+\nabla\cdot\lambda_{dw}-\frac{\partial(\varphi p_w)}{\partial t}-\mathbf{u}_\mathbf{w}\nabla p_w-q'_w h'_w=0 \quad (39)$$ For the liquid phase: $$\frac{\partial\left[\left(1-\phi\right)\rho_r h_r\right]}{\partial t}+\nabla\cdot\lambda_{cr}=0 \quad (40)$$ Where h is the specific enthalpy, λ_c is the heat conduction vector, and λ_d is the dispersion vector. Description of heat transport in the system: $$\left[\phi\rho_w c_w+\left(\left(1-\phi\right)\rho_r c_r\right)\right]\frac{\partial T}{\partial t}-\nabla\cdot\left(K_m\nabla T\right)+\rho_w c_w\mathbf{u}_\mathbf{w}\nabla T=0 \quad (41)$$ Where c_w and c_r are the specific heat of water and rock, and K_m average thermal conductivity. The geomechanics of the system is: $$\rho\frac{\partial^2 u}{\partial t^2}-\nabla\cdot\sigma-\rho g-\alpha\nabla p-\beta K\nabla T=0 \quad (42)$$ With u the displacement vector, α the effective biot stress, and β the coefficient of thermal expansion, this equation provides the stress equilibrium for the hydrothermomechanical problem.
COMSOL-Multiphysis [34,35] Computer Model Solution	General theory of single-phase flow: $$\frac{\partial\rho}{\partial t}+\nabla\cdot\left(\rho\mathbf{u}\right)=0,\ \frac{\partial\mathbf{u}}{\partial t}+\rho\left(\mathbf{u}\cdot\nabla\right)\mathbf{u}=\nabla\cdot\left[-p\mathbf{I}+\mathbf{K}\right]+\mathbf{F} \quad (43)$$ $$\rho C_p\left(\frac{\partial T}{\partial t}+\left(\mathbf{u}\cdot\nabla\right)T\right)=-\left(\nabla\cdot\mathbf{q}\right)+\mathbf{K}:\mathbf{S}-\frac{T}{\rho}\frac{\partial\rho}{\partial t}\bigg|_p\left(\frac{\partial p}{\partial t}+\left(\mathbf{u}\cdot\nabla\right)p\right)+Q \quad (44)$$ With ρ as the density, **u** the velocity vector, p the pressure, **I** the identical matrix, **K** the viscous stress tensor, **F** the volume force vector, Cp the heat capacity, T the absolute temperature, **q** the heat flux vector, Q the heat source, and **S** the strain rate tensor. The momentum equation for compressible flow: $$\rho\frac{\partial\mathbf{u}}{\partial t}+\rho\mathbf{u}\cdot\nabla\mathbf{u}=-\nabla p+\nabla\cdot\left(\mu\left(\nabla\mathbf{u}+\left(\nabla\mathbf{u}\right)^T\right)-\frac{2}{3}\mu\left(\nabla\cdot\mathbf{u}\right)\mathbf{I}\right)+\mathbf{F} \quad (45)$$ Where μ is the viscosity. Heat transfer interfaces: $$\rho C_p\left(\frac{\partial T}{\partial t}+\mathbf{u}_{trans}\cdot\nabla T\right)+\nabla\cdot\left(\mathbf{q}+\mathbf{q}_r\right)=-\alpha T\frac{dS}{dt}+Q \quad (46)$$ Where $\mathbf{u}_{trans}$ is the translational velocity vector, **q** is the conductive heat flux, $\mathbf{q}_r$ is the radiative heat flux, α is the coefficient of thermal expansion, and S is the second Piola-Kirchhoff stress tensor. Heat transfer in fluids:

Table 2. *Cont.*

SOFTWARE/CODE	MODELS/SOLUTION OF EQUATIONS BASE
	$$\rho C_p\left(\frac{\partial T}{\partial t}+\mathbf{u}\cdot\nabla T\right)+\nabla\cdot\left(\mathbf{q}+\mathbf{q}_r\right)=-\alpha_p T\left(\frac{\partial p}{\partial t}+\mathbf{u}\cdot\nabla p\right)+\tau:\nabla\mathbf{u}+Q \quad (47)$$ The model mechanical and hydraulic processes are coupled with: $$\rho S\frac{\partial p}{\partial t}+\nabla\cdot\left[\rho\left(\mathbf{q}=-\frac{k}{\mu}\nabla p\right)\right]=Q-\rho\alpha\frac{\partial\varepsilon_v}{\partial t} \quad (48)$$ With volumetric strain tensor ε_v, pore pressure p, Biot constant α, Darcy velocity $\mathbf{q}$, permeability k, fluid dynamic μ, storage parameter S, and fluid source/skin-term Q.
CMG-STARS [36] Computer Modelling Group Ltd	The relationship of the effective shear of the porous medium and the fluid velocity: $$\dot{\gamma}=\frac{\left(\gamma_{fac}=C\left[\frac{3n+1}{4n}\right]^{\frac{n}{n-1}}\right)\left\|\mathrm{u}_1\right\|}{\sqrt{\mathrm{kk}_{r,1}\phi S_1}} \quad (49)$$ Where k is the permeability, ϕ the porosity, $\mathrm{u_l}$ the Darcy velocity, $\mathrm{k_{r,l}}$ the relative permeability, S_l the saturation, pseudoplastic shear, and C constant 6n n=0.5. Intrinsic fracture porosity: $$\varphi_f=1-F_{fr}\cdot\left(1-\varphi_{fr}\right) \quad (50)$$ F_{fr} fracture fraction, and ϕ_{fr} is the formation porosity. Fracture void volume: $$V\cdot F_f\cdot\left(1-F_{fr}\right) \quad (51)$$ Total volume of formation pores (matrix plus fractures): $$V\cdot\left(1-F_f\right)\cdot\varphi_r+V\cdot F_f\cdot F_{fr}\cdot\varphi_r=V\cdot\varphi_r\cdot\left[1-F_f\cdot\left(1-F_{fr}\right)\right] \quad (52)$$ Where φ_r the intrinsic formation porosity, and V the gross volume. Permeability function of fluid porosity: $$k=k_0\cdot\exp\left[k_{mul}\cdot\left(\frac{\phi-\phi_0}{1-\phi_0}\right)\right] \quad (53)$$ With k_0 and ϕ_0 being the initial fluid permeability and porosity, and k_{mul} being the user-defined factor. The mechanics of dispersive flow of component i in phase j in the k direction: $$J_{ijk}=-\varphi S_j\alpha_{jk}\left|u_j\right|\nabla_k\left(\rho_j X_{i,j}\right) \quad (54)$$ With ϕ porosity, S_j saturation of phase j, α phase dispersivity for phase j in the k direction, u_j phase velocity magnitude, $\nabla_k(\rho_j X_{ij})$ concentration gradient of component i in phase j in the k direction.
OpenGeoSys OGS [37,38]	The governing equations for hydraulic and thermal processes implemented in OGS for a fractured medium are respectively: $$Q_f=eS_s^f\frac{\partial p}{\partial t}-\overline{\nabla}\left(\frac{k^f}{\mu}\left(\overline{\nabla}p+\rho^f g\right)\right),\ Q_T=e\rho^f c_p^f\frac{\partial T}{\partial t}+e\rho^f c_p^f v\cdot\overline{\nabla}T-\nabla\left(e\lambda^f\overline{\nabla}T\right) \quad (55)$$ The fluid discharge, Q_f, can be either a sink or source, e is the fracture apertura, S_s^f is the fracture specific storage, p is the fluid pressure, t is time, k^f is the fracture permeability, μ is the dynamic viscosity, ρ^f is the density of the fluid, and g is the gravity acceleration, heat transport, Q_T is either a source or sink, c_p^f is the specific heat capacity of the fluid, T is the temperatura, v the Darcy's velocity, and λ^f the heat conductivity of the fluid. The governing equations for the heat transport in a porous medium: $$\left(c\rho\right)^{eff}\frac{\partial T}{\partial t}+\left(cp\right)^{fluid}\mathbf{v}\cdot\nabla T-\nabla\cdot\left(\lambda^{eff}\nabla T\right)=q_T$$ $$\left(c\rho\right)^{eff}=\sum_\alpha\varepsilon^\alpha c^\alpha\rho^\alpha\ ,\ \left(c\rho\right)^{fluid}=n\sum_\gamma S^\gamma c^\gamma\rho^\gamma\ ,\ \lambda^{eff}=\sum_\alpha\varepsilon^\alpha\lambda^\alpha \quad (56)$$ With c the specific heat capacity, T temperature, t time, $\mathbf{v}$ the Darcy velocity, λ^{eff} the effective thermal conductivity of a porous media, q_T heat production, ρ density, α all phases, γ fluid phases, ε^α the volume fraction of the phase α, and n porosity. Darcy law for each fluid phase γ in multiphase flow: $$\mathbf{q}^\gamma=nS^\gamma\mathbf{v}^\gamma=-nS^\gamma\left[\frac{k_{rel}^\gamma\mathbf{k}}{\mu^\gamma}\left(\nabla p^\gamma-\rho^\gamma\mathbf{g}\right)\right] \quad (57)$$

3. Results and Discussion

3.1. Capabilities and Limitations of Simulators

In keeping with the title and objective, a review was developed for the recognition of codes, and software associated with coupled processes involving fluid flow, heat transfer, and stress deformation, as a resource for various processes in earth sciences that are intrinsically coupled, especially in the thermal, hydraulic, and mechanical fields. But whose effects, until now, can only be examined through numerical models. For example, research into HDR systems has evolved, with a high level of active interest in the development of numerical models, as shown in this bibliographic review.

To date, there is no unified code that couples general Thermo-Hydro-Mecha-Chemical processes, (including multiphase, and multicomponent fluid flow and reactive transport) in geological media [1]. This evaluation pertains to formulation of the Thermo-Hydro-Mechanical process [6,16], describes heat transfer, fluid flow, and rock matrix mechanics during cold fluid injection and hot fluid production.

For this they have used the coupling of existing codes, each one specialized in some of the four processes involved, and thus generate more robust solvers. For example, AUTOUGH2 has been coupled with ABAQUS, to analyze advanced constitutive behaviors in large 3D simulations for equilibrium at every time step [39]. The work by Zyvoloski indicates that FEHM differs from TOUGH2, and NUFT (Nonisothermal Unsaturated-Saturated Flow and Transport model) in using Newton-Raphson iterations [30], because the derivatives are formed analytically rather than numerically, leading to faster convergence of stiff nonlinear equations. Although FEHM itself is coupled with PEST (Parameter ESTimation), and optimizes with AMALGAM (approach a multialgorithm, genetically adaptive multiobjective), it does not have the disadvantage of speed, graphical interface and packages on complex contours like MODFLOW.

FRACTure is based on the DLEARN code, with routines, and libraries for linear static and dynamic finite element análisis [3]. TOUGH2 with THC, and FLAC3D has been linked for nonlinear functions in geothermal processes, oil and gas reservoirs, contaminant migration, and nuclear waste isolation, and with TOUGHREACT for reactive transport in mineral dissolution [1].

For isothermal problems in shallow reservoirs such as MOCDENSE with PHREEQE (PH REdox EQuilibrium), and reactive transport problems 3DHYDROGEOCHEM, TOUGH2/EWASG, CHEM-TOUGH2, and TOUGHREACT that use empirical approaches, or simplified geometric derivations valid only for restricted cases [8]. SHEMAT has greater coupling relations, and implements a fractal approach, so the permeability is obtained by a series of porosity, and the same permeability is estimated by complementary petrophysical, and petrographic methods.

GEOSIM, TERASIM-THER has been incorporated as a 3D three-phase simulator, for isothermal or thermal flow with FEM3D (Finite Element Method 3D) of poroelastic, and thermoelastic characteristics in the analysis of stresses, and deformations in porous rocks, and soils. GEOFRAC in the fractured interface of the reservoir [24]. For processes where single-phase phase boiling does not occur, SHEMAT and FEFLOW have been effective [40]. In relation to observed, and field monitoring, laboratory tests and soil column tests, COMSOL validates these attributes [41].

Individual solutions have also been obtained, and compared with analogous simulators as STAR, and NIGHTS (Nonequilibrium Incompressible Geotherms Heat Transfer Simulator), with the same initial conditions [42]. IPARS has been successfully implemented using a PETS solver, for linear systems. The general minimum residual method GMRES (Generalized Minimal Residual Method), and with LU (Lower-Upper) factorization [27].

As IPARS can map faults, and can be run in different domains of a reservoir, it has allowed a combination with JAS3D, as it handles large sliding contact surfaces, and non-linear inelastic deformations. In addition to linearizing with GMRES, and comparing with the ARCO, and ACRES simulator, showing similarity [28]. In other cases, for example, it has been recognized that FRACSIM-3D does not implement fluid physics, water/water interaction, temperature-dependent fluid viscos-

ity, turbulent fluid flow, shear shadow effects or well impedance [26], which leads to estimating data, although derivation with field data is better.

For hydraulic fracturing simulation, FRACCSM, TOUGH2-CSM, SUNGAS, Elfen, Kinetix Stimulation, ResFrac, Resfrac, @Frac, Thermal EDFM, Xsite 4.0, MFrac, Fracman, FracCADE, FracPro have been used. According to the Environment Agency [43], most of them use the fracture propagation criterion (HYFRAC, TerraFrac, TRIFRAC, MFRACII, ENEFRAC, StimPlan), and others use tensile strength (GOHFER and FracOptima). In this review, the factors that most affect fracture dimensions are: in-situ stress, stratum thickness, Young's modulus, Poisson's ratio, fracture toughness, injection rate and injected volume, fluid viscosity, leakage rate, and the pre-existing fracture network.

In this way [9], the interaction of hydraulic, and natural fractures is not fully resolved, thus natural fracture properties are affected by hydraulic fractures, although hydraulic fracturing models are used to investigate specific mechanisms rather, than design hydraulic fracturing treatments, and the input parameters, boundary conditions and numerical scales are not as realistic, as commercially available simulators.

3.2. Features and Application Cases

Given the recent studies of coupled systems, and the implementation of computational solvers, **Table 3** shows a summary of some characteristics of each code/software, as well as recent application cases [1,8,20,21,25–38,44–56].

Simulators can be used to model EGS, and among the most notable are for hydrothermal reservoirs: TOUGH2, TETRAD, STAR, FEHM, for HDR reservoirs: FRACTure, GEOCRACK, GEOTH3D and FRACSIM-3D. New simulators based on TOUGH2 and other codes with modern programming languages and integrated parallelization are currently being developed, such as: OpenGeoSys and FALCON or others as DuMu, PFLOTRAN and STOMP [20–22,28–30,40].

Table 3. Main Features, and Case Applications of the Coupling Codes, and Software Associated with HDR EGS (Own Elaboration).

Code or Software	Some Features	Application Cases
TETRAD	Written in FORTRAN 77, for dark oil, multicomponent (water, gas, and oil), thermal and geothermal, dual porosity-permeability. Supported with Newton-Raphson iterations. Has been validated against comparative problems, with geothermal codes. The numerical results obtained can be compared with analytical results [20].	TETRDAD has been used with data from Brady Hot Springs in Nevada, USA, and a 10-well synthetic geothermal system. A high level of accuracy was achieved in the predictions of these systems, even with 80–101 simulations. The relative error of 4.75% was observed across all pressure, temperature, and energy predictions studied [44].
TOUGH2	Numerical simulator for non-isothermal multicomponent and multiphase fluid flows in one-, two-, and three-dimensional porous and fractured media. Applications in geothermal reservoir engineering, nuclear waste disposal, environmental assessment and remediation, and hydrology of saturated and unsaturated zones. Conjugate gradient solvers are included for more efficient solution delivery. Written in the FORTRAN77 standard for physical process analysis, modeling, and mathematical and numerical methods [25].	Study on reservoir stimulation and thermal extraction in the Qiabuqia, China. With a three-well horizontal; an injection, two productions. Spacings of 300 m for the minimum case, 400 m, 500 m for relatively large natural fractures and 600 m for the maximum. The horizontal well trajectory is a 1,500 × 1,000 × 500 m model at depths between 3,300 and 3,800 m. Initial reservoir temperature is T = 190.0–0.071z (°C) and initial reservoir pressure is P = 3.3×10^7–10000z (Pa). Because the surrounding rocks with extremely low permeability (2.6×10^{16} m^2) are not fractured [45].
FRACTure	Discrete fractures, finite element coding, coupled hydraulic-thermal and mechanical simulation. Represents fluid flow in impermeable rock matrix, uses Darcian and turbulent models. Applies effective thermoelasticity, and poroelasticity. Heat transfer includes conduction in the rock, and transport in the fluid, coupled to the elastic and thermal solutions. Used to compare simulations using single, and multiple fractures in 2D or 3D. Not include two-phase flow or coupling geochemistry to flow [21].	Soultz field with four operating and monitoring wells. Initially, well GPK1 at 3,600 m and exploration well EPS1 at a depth of 2 km. Well GPK2 at 3,880 m, wells GPK3 and GPK4 at over 5,000 m. The three deep wells are separated by 650 m at a depth of 5 km. GPK1 and GPK2 are separated by 450 m of granitic rocks. The granitic basement is reached at only 1,400 m depth. Mesh sizes in the immediate vicinity of the wellbore are smaller than 3 m. Beyond the wellbore, they are 40 m, increasing to 500 m in the far field [46].

Table 3. *Cont.*

Code or Software	Some Features	Application Cases
FRACSIM-3D	Code for fluid flow and heat transfer, including fracture shear and dilation during stimulation and circulation, thermoelasticity during circulation, chemical dissolution and precipitation [26]. Convective heat transfer based on fracture networks. The simulator facilitates the effects of stimulation, and fluid circulation on fracture shear stress. It simulates changes in thermoelastic properties, and chemical changes due to fluid circulation [47].	The Hijiori and Soultz reservoirs were modeled, including circulating fluid fracture network topologies, and heat transfer. Seismic data were used to determine proportional non-uniform porosity [47].
TOUGH-FLAC3D	Coupling in multiphase fluid flow analysis, injection and storage problems in unsaturated porous media. FLAC3D is developed for rock, and soil mechanics, and coupled thermomechanical, and hydromechanical processes for single-phase fluid flow. TOUGH2 and FLAC3D for modeling THM processes in porous, and fracturated geological media. They run sequentially on compatible numerical grids, and are linked through external docking modules [1].	Study of an ATES system in Shanghai, China, with four water wells for seasonal heating, and cooling of an agricultural greenhouse, at a depth of 74–104.5 m, alternating sand and silty sand layers, and clay cover. Groundwater level, temperature, and ground subsidence data from 2015–2017 were collected from field monitoring. Was implemented a thermoelastoplastic constitutive model. The effectiveness of the numerical model was validated with field data. The model reproduced groundwater flow, heat transfer, and mechanical responses in porous media to assess heat- and pressure-induced ground subsidence [48].
SHEMAT	Reactive transport simulation code for thermal and hydrogeological problems in two and three dimensions. It solves coupled problems: fluid flow, heat transfer, species transport, and water-rock chemical interactions in fluid-saturated porous media. It covers a wide range of time scales. It models both stationary, and transient processes in hydrogeothermal reservoirs. It covers the transport of dissolved species, geochemical reactions between the solid, and fluid phases, and extended coupling between individual processes (porosity and permeability) [8].	Comparison of SHEMAT-Suite with the numerical solution of the Theis model. The grid is coarser away from the wellbore, and finer in the center. With a pumping well, time-step control, and transient simulation with default values. The simulation runs for 3.5 days. The Dirichlet boundary conditions for the lateral head are set to 20 m, and the upper and lower parts of the model are not flow boundaries. The sump is specified as a pumping rate of $-0.001\ m^3s^{-1}$. The initial hydraulic head is set to 20 m. The fluid density is 1000 kg m^{-3}, the compressibility is 5×10^{-8} $ms^{-2}\ kg^{-1}$, and the viscosity is 10^{-3} $kgm^{-1}\ s^{-1}$. For the rock matrix, properties include porosity (10%), permeability ($10^{-12}\ m^{-2}$) and compressibility ($10^{-8}\ ms^{-2}\ kg^{-1}$) [49].
IPARS	For very large linear elasticity and nonlinearities, running in parallel for one and two phases, water-oil, air-water, and reactant transport. With implicit equation of state composition for large-scale reservoirs. It contains several numerical discretizations: mixed finite elements and discontinuous Galerkin finite elements for two-phase flow. It allows for discontinuity, and degeneracy of fluid-rock properties, and features optimal convergence properties. It implements different time discretizations: implicit, semi-implicit, and sequential [27,28].	Field-scale CO_2 sequestration pilot project at the Cranfield deposit, located in Mississippi, USA, a salt-dome geological structure. By 2015, approximately 0.5 million metric tons of CO_2 had been injected. The reservoir model includes 2194 m deep. Five injection wells were simulated under no-flow boundary conditions, and eight pseudoproduction wells were assigned to the reservoir boundaries to simulate open boundary conditions. A constant bottomhole pressure equal to the initial reservoir pressure of 4650 psi, and the initial reservoir temperature was 125 °C. The reservoir was initially assumed to be saturated with brine [50].
MOTIF	Solution of governing equations: equilibrium, subsurface flow, heat transport, and conservative and non-conservative solute transport in fractured porous media. 3D finite element code simulates coupled/uncoupled steady-state or transient, with discrete fractures represented. Thermo-Hydro-Mechanical [29].	To predict the hydrogeological disturbances caused by the excavation of the URL (Underground Research Laboratories, AECL Atomic Energy of Canada Limited) well to a depth of 255 m. The predicted drawdown histories agreed satisfactorily with measurements. The observed seepage in the well also agreed with predictions. The magnitude of the seepage rate was overestimated by a factor of three. Discrepancies may include the difference between the assumed, and actual excavation model, the presence of vertical fractures, and the reduction in hydraulic conductivity near the excavation [29].

Table 3. *Cont.*

Code or Software	Some Features	Application Cases
FEHM	Complex subsurface coupling in hydrology, geothermal energy, and petroleum; solution of nonlinear equations, such as mass and energy balance, advection, and dispersion, reactive coupling, thermo-hydrological, and mechanical processes; finite element and finite volume handling in FORTRAN 90; use of modules and subroutines. It uses analytical derivatives in Newton-Raphson iterations, with dual porosity methods. It has been compared with TOUGH2 and MODFLOW [30,31].	Simulated FEHM results have been used for ANN (artificial neural network) modeling, as training, validation, and testing data. The random approach has been employed. The ANN input variables are local temperatures, pressures, mass flow, and fracture transmissivity along the fracture plane. The ANN output is the temperature in the production wellbore. A transfer function is required, for hidden layers and a linear activation function, for the output layer. Statistical methods such as square root error are used [51].
HYDROTHERM	Multiphase simulator for groundwater flow associated, with thermal energy and transport, spatial and temporal discretization with finite differences, for groundwater flow, considering water-vapor capillarity. Ability to simulate unconfined groundwater flow with precipitation-recharge boundary conditions, ground surface seepage, iterative solver for linear equations (generalized least residual method), time- or depth-dependent functions for permeability, dynamic matrix assignment, graphical user interface for input and output [32].	Application of the code on the islands of Gran Canaria, Lanzarote, and Tenerife. The former has a normal geothermal gradient, the latter has magmatic bodies near the surface, and Tenerife has recharge and discharge flows. On the first two islands, drilling was required to adjust and validate the models, while Tenerife used the same methodology but without verification drilling. This code has great potential for determining the most suitable location, for deep exploration drilling. The main advantage is its ability to reliably reproduce different evolutionary, and case-specific models using the same geological and thermal parameters [52].
FALCON	Flexible, modular systems for physics, materials properties, boundary conditions, unstructured grid with many element types, hybrid parallelism that scales, error estimation, parallel physics, coupled multi-scale modeling, fracture simulation, fluid flow, rock deformation, heat transport, complex coupled thermoporoelastic problem, interaction fluid-rock [33]. It has been validated through various benchmark problems; source code is open source [53].	Native State Reference Model at FORGE Utah. The conceptual, and ground models of the reservoir were used numerically to estimate the spatial distribution of natural pressure, temperature, and stress conditions for planning FORGE operations. The numerical implementation included complex boundary conditions, and a three-dimensional parameter distribution. The FORGE numerical model domain consists of the site's pilot well, and future injection, and production wells. The domain measures 2.5 km × 2.5 km × 2.75 km, and ranges in depth from 400 m to 3,200 m. The lithology was divided into granitic basement rocks (granitoid), and sedimentary fill deposits [53].
COMSOL-Multiphysis	Fluid dynamics, geomechanics, heat transfer, fluid mixing, flow in porous media, thermodynamics, transport phenomena, among others. Finite elements, in fluid flow interfaces, laminar, and turbulent flow, porous media interfaces, heat transfer in solids, liquids, solids-liquids, non-isothermal flows, stabilization methods, fluid-solid interactions, solid interfaces, solute transport. Includes: stationary and time-dependent (transient) studies, linear, and nonlinear studies, and natural frequency, modal, and frequency response studies [34,35].	A 2D numerical model was solved in a 300 m × 300 m single-fracture thermal reservoir to check accuracy. Fractures are randomly generated using a powerlaw distribution with an index of 2, and sizes between 30 and 50 m, with 300 fractures oriented 30° and 135°. The fracture temperature distribution after 200 days was compared numerically, and analytically. Temperature changes are compared at various positions within the fracture (x = 20 m, 40 m and 60 m) as a function of time. The numerical, and analytical solutions show very high agreement, with a maximum relative error of 3.44%. The fracture flow, and heat transfer simulation implemented in COMSOL is accurate, reliable, and feasible for numerical simulation investigation in EGS [54].

Table 3. *Cont.*

Code or Software	Some Features	Application Cases
CMG-STARS	Coupled processes by finite difference/finite element grids with hybrid orientations, multi-component, three-phase thermal, and steam additive simulator. Meshes can be Cartesian, cylindrical, or variable depth/thickness. Stabilized dispersions (droplets, bubbles and films), components (including adsorption, blocking, nonlinear viscosity, dispersion and mass transfer in non-equilibrium situations). Flow in naturally fractured reservoirs can be simulated using four different models: dual porosity, dual permeability, multiple interaction continuums, or vertical refinement [36].	The model volume is 2000 × 1000 × 3800 m, with 40 × 20 × 38 grid blocks. From 3200 m to 3700 m depth, they were refined five times horizontally, and three times vertically. With three vertical wells, injection located in the center, and two production wells, spaced 500 m apart. With five hydraulic fractures, with an average length of 483 m, a height of 100 m, a width of 3 mm, and an average permeability of 36,000 mD. The solver's convergence criterion is set to 1×10^{-6}, to limit the mass balance error to less than 0.001%, of the water injected into the target area. The mesh block dimensions were halved in all directions in a mesh refinement study, and results show that a variance of less than 0.2% is achieved [55].
OpenGeoSys OGS	Capability to model coupled hydraulic, and thermal processes (TH), open source for the numerical simulation of thermohydromechanical/chemical (THMC) processes in porous, and fractured media. It is targeted at applications in environmental geoscience, contaminant hydrology, water resource management, waste repositories or geothermal systems, or energy storage. It features a flexible numerical framework using Finite Element Method interfaces for pre- and post-processing. Heterogeneous, or fractured porous media can be managed using continuous, or discrete dual approaches, by coupling elements of different dimensions [37,38].	Model validation with analytical solutions, and simulation over a 30-year long injection period. When thermal reduction occurs, productivity degrades rapidly. Hydraulic fractures are simulated with sufficiently large fluid pressures, to overcome the normal stresses exerted on the fracture faces. Submodels are assembled using a pure FEM approach. Incorporating frictional slip between fracture faces, tensional hydraulic fracture opening played an important role in controlling the spatiotemporal distribution of induced seismicity [56].

3.3. Implications of THGMC Coupling

As reviewed, the data that most simulators require are:

(a) Porous/fractured medium: location, geological formation, morphology, lithology, density, porosity, permeability (maximum, minimum and effective) of natural fractures, Young's modulus, Poisson's ratio, compressibility of the rock bulb, pore pressure, fracture pressure, burial stress, fracture tortuosity, fracture spacing, fracture aperture, length, height, stresses (maximum, minimum and effective) and their direction, water saturation, cohesion, friction angle, shear stress, wettability, damage, tensile strength, and fluid loss coefficient.

(b) Heat flow: depth, surface temperature, bottom temperature, heat flow, geothermal gradient, thermal conductivity, isobaric heat capacity, thermal diffusivity, and enthalpy.

(c) Fluid Flow: density, specific heat, pressure, temperature, enthalpy, viscosity, salinity, liquid compressibility, flow rate, and leakage coefficient.

(d) Well: location, geometry, depth, pressure head, radius, temperature of outer walls, boundaries, injection pressure, and reference depth.

(e) Phase interaction: thermal conductivity of the mixed phase, thermal conductivity of the reservoir, thermal conductivity of the water phase, relative permeability, coefficient of thermal expansion, and phase viscosity.

In various studies, the same codes can simulate in a coupled or uncoupled manner, in steady or transient state, in fractured or deformable porous media. Since most of them include the equilibrium equation, the flow equation, the heat transport equation, and the solute transport equation [29]. In addition to the basic features of conventional geothermal, and geomechanical simulators, explicit representation of fractures, fracture aperture changes due to effective and shear stress, thermoelastic effects, relationship between fracture aperture and conductivity, fluid flow channeling with fracture, water-rock chemical reactions, and well-reservoir coupling are required [21].

The wide variety of codes or software incorporate

coupling, some with high levels of sophistication, by considering induced disturbances from hydraulic, mechanical and thermal effects as shown in **Figure 2** [41]. HDR EGS system, by the injection of cold fluid flow into a hot reservoir, and its cooling by the stresses above the production temperature, due to conduction and advection.

THGMC conceptual model of **Figure 2** shows that there is a strong relationship between Geology, Thermodynamics, Hydraulics, Mechanics and Chemistry for EGS, and each area contributes with its basic formulations, principles and constitutive relationships, as shown in **Table 2**. Although models have also been found in a duo-coupled: as the Geothermal, Geohydraulic, Geomechanical and Geochemical cases, with tri-coupling the Thermo-Hydro-Mechanical and Thermo-Hydro-Mechanic-Chemical cases, and in this research Thermo-Hydro-Geo-Mechanic-Chemical is incorporated (on geological systems G, not incorporated in other conceptual models), of THGM interest for future research on EGS in HDR.

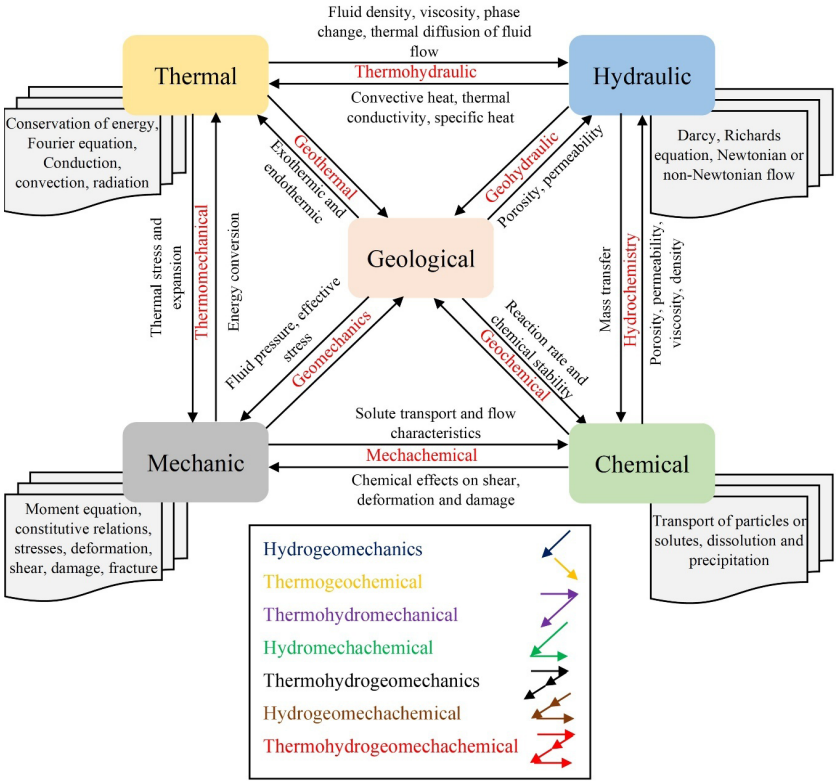

Figure 2. Relations in the Field of ThermoHydroGeoMechaChemical Coupling, THGMC Conceptual Model (Own Elaboration Based on Work by Li and Yin) [41].

But, as has been reviewed, there is greater weight on the Geomechanical part, because the current models are based on mechanics (deformation due to temperature changes, injection or production), discrete fracturing, critical shear, effective stresses and even empirical permeability, which according to may increase during injection, but in closures may decrease, therefore cyclic injection models are necessary for reversible permeability [39].

When the injection stops, and the fluid pressure returns to the natural state level, the permeability decreases due to a combination of factors as: (i) chemical, if the greater the salinity of the fluid, the lower the decrease in permeability, mineral precipitation, changes in state or particle deposition, (ii) hydrodynamic, due to the presence of a critical injection flow rate, above the permeability, causing the release of frictional particles, and (iii) mechanical, such as obstruction of pores by injected fluids, changes in the stress state of the rock, and turbulence effects. However, the damage to the rock matrix is permanent, and therefore a part of the improved permeability is also permanent, but it is

not clear if this relationship is adequate [39], therefore it is necessary to calibrate, and test with short-term experimental data the models that various authors have proposed.

By assuming behaviors as poroelastic in the formations, the structural-mechanical response to the pumping, and injection regime can be very low, and the external hydraulic gradient less than the pumping effect [35], being highly complex due to the geological properties.

In this way, every coupled system must consider the hydraulic field provided, by the source through the injection well to the fracture network of the reservoir, as the thermal field, returning through the extraction well as a sink. Although, it is worth noting that the same codes do not fully consider, the possible leakage of fluid flow towards the matrix, and the heat loss based on the movement of the same flow, given that particles at low speeds acquire greater heat transfer and vice-versa, in addition to the friction losses in the generation of local heat sources.

To accurately solve the equations, methods such as finite differences, finite elements, finite volumes, discrete or equivalent methods, and the recent implementation of fractal and fractional methods have been used. The latter are more relevant for future improvements in software development, as they are more realistic. However, it might be more beneficial to make greater efforts to improve, validate, and verify existing codes in relation to experimentation, and their application in large-scale and relevant projects [29].

There is still no numerical model that unifies the four disciplines, and they depend on a single variable. The complexity involved is recognized, but recognizing the mathematical formulations allows us to conceive and differentiate the attributes that each simulator incorporates.

4. Conclusions

Current codes and software associated with fluid flow, heat transfer, stress deformation and reaction changes are purely non-linear and extremely complex processes. Systems of multi and interdisciplinary interest, with highly coupled processes such as Thermo-Hydro-Geo-Mecha-Chemical.

The continuity equation, energy, momentum, and transfer remain the basic formulations in this type of simulator. Additionally, the Fourier equation is used for the thermal component, Darcy's Law for hydraulics, and constitutive relations for mechanics, and solute transport in chemistry, mainly. The current numerical solution schemes used are finite difference, finite element, finite volume, or fractional fractal methods.

The numerical and modular structures of the codes and software are highly rigorous, providing greater precision for real-world processes. Although with some flexibility that allows the user to identify, and manipulate to incorporate linear, and non-linear physical processes when recognizing the formulations.

The main data required by most simulators are: porous/fractured: geological formation, morphology, lithology, density, porosity, permeability, Young's modulus, Poisson's ratio, fracture pressure, stress, aperture, length, and damage. For heat flow: bottomhole temperature, heat flux, thermal gradient, conductivity, heat capacity, diffusivity, and enthalpy. For fluid flow: pressure, viscosity, salinity, compressibility, flow rate, and storage coefficient. As well as well data, and data on liquid-vapor phase interaction due to temperature changes.

There is still no universally coupled code that incorporates fluid flow, heat transfer, and stress deformation. However, the appropriate choice for simulating such processes will depend on the availability of data, parameters, or input information. Such as pressure, seismic, gravimetric, geophysical, petrophysical, geomechanical and geochemical tests.

The starting point could be to analyze systems as single-coupled systems, then as duo-coupled systems, and finally as tri-coupled systems, to interpret processes, and their constituent subprocesses. This would allow for the identification of hydraulic flow losses, heat losses, and residual fracturing mechanisms, in addition to the effects of friction, and turbulence, which have been poorly studied in current simulators.

Currently, supercomputers are available as tools for preprocessing, solving, and postprocessing mathematical expressions that rely on numerical methods, such as those available in these software packages. The field of research for this type of highly complex phe-

nomena, such as THGMC, is broad.

Funding

This work was supported by Secretaría de Ciencia, Humanidades, Tecnología e Innovación de México, as part of the research on hot dry rock enhanced energy systems grant number [8085107].

Institutional Review Board Statement

Not applicable.

Informed Consent Statement

Not applicable.

Data Availability Statement

Data from this review are available in publications, code manuals, and software.

Acknowledgments

The author would like to thank the Secretaría de Ciencia, Humanidades, Tecnología e Innovación de México, as well as the Division of Earth Science Engineering, Faculty of Engineering of the UNAM for the support provided during the research.

Conflicts of Interest

The author declares no conflict of interest.

References

[1] Rutqvist, J., Wu, Y.S., Tsang, C.F., et al., 2002. A modeling approach for analysis of coupled multiphase fluid flow heat transfer, and deformation in fractured porous rock. International Journal of Rock Mechanics and Mining Sciences. 39(4), 429–442. DOI: https://doi.org/10.1016/S1365-1609(02)00022-9

[2] Swenson, D., DuTeau, R., Sprecker, T., 1995. Modeling flow in a jointed geothermal reservoir. Proceedings of the World Geothermal Congress; 18–31 May 1995; Florence, Italy. pp. 2553–2558.

[3] Kohl, T., Hopkirk, R.J., 1995. FRACTure – a simulation code for forced fluid flow and transport in fractured, porous rock. Geothermics. 24(3), 333–343. DOI: https://doi.org/10.1016/0375-6505(95)00012-F

[4] Labus, K., Labus, M., Lesniak, G., 2023. Thermal properties of rocks from deep boreholes in Poland in terms of obtaining geothermal energy from enhanced geothermal systems. Advances in Geo-Energy Research. 8(2), 76–88. DOI: https://doi.org/10.46690/ager.2023.05.02

[5] Abid, K., Sharma, A., Ahmed, S., et al., 2022. A review on geothermal energy and HPHT packers for geothermal applications. Energies. 15(19), 7357. DOI: https://doi.org/10.3390/en15197357

[6] Yan, B., Gudala, M., Sun, S., 2023. Robust optimization of geothermal recovery based on a generalized thermal decline model and deep learning. Energy Conversion and Management. 286, 117033. DOI: https://doi.org/10.1016/j.enconman.2023.117033

[7] Gao, X., Li, T., Zhang, Y., et al., 2022. A review of simulation models of heat extraction for a geothermal reservoir in an enhanced geothermal system. Energies. 15(19), 7148. DOI: https://doi.org/10.3390/en15197148

[8] Clauser, C., 2003. Numerical simulation of reactive flow in hot aquifers SHEMAT and processing SHEMAT. Springer-Verlag: Berlin, Germany. pp. 339.

[9] Chen, B., Ramos, B.B., Sun, Y., et al., 2022. A review of hydraulic fracturing simulation. Archives of Computational Methods in Engineering. 29, 1–58. DOI: https://doi.org/10.1007/s11831-021-09653-z

[10] Nemat-Nasser, S., Ohtsubo, H., 1978. Fluid flow and heat transfer through hydraulically induced fractures in hot, dry rock masses. Journal of Pressure Vessel Technology. 100(3), 277–284. DOI: https://doi.org/10.1115/1.3454467

[11] Zhang, Q., Dahi, T.A., 2023. Autonomous fracture flow tuning to enhance efficiency of fractured geothermal systems. Energy. 281, 128163. DOI: https://doi.org/10.1016/j.energy.2023.128163

[12] Wang, Y., HosseiniMehr, M., Marelis, A., et al., 2023. A generic framework for multiscale simulation of high and low enthalpy fractured geothermal reservoirs under varying thermodynamic conditions. Energies. 16(2), 928. DOI: https://doi.org/10.3390/en16020928

[13] Liu, S., Dahi, T.A., 2023. Factors affecting the efficiency of closed-loop geothermal wells. Applied Thermal Engineering. 222, 119947. DOI: https://doi.org/10.1016/j.applthermaleng.2022.119947

[14] Liu, S., AlBalushi, F., Dahi, T.A., 2023. Conductive proppants to improve heat extraction. Proceedings of the 48th Workshop on Geothermal Reservoir Engineering; 6–8 February 2023; Stanford, CA, USA. pp. 1–7.

[15] Santos, L., Dahi Taleghani, A., 2023. Impact of

microannulus on the efficiency of heat transfer in the bottomhole. Frontiers in Energy Research. 11, 1–8. DOI: https://doi.org/10.3389/fenrg.2023.1142662

[16] Yan, X., Xue, K., Liu, X., et al., 2023. A novel numerical method for geothermal reservoirs embedded with fracture networks and parameter optimization for power generation. Sustainability. 15(12), 9744. DOI: https://doi.org/10.3390/su15129744

[17] Abdelhafiz, M.M., Oppelt, J.F., Brenner, G., et al., 2023. Application of a thermal transient subsurface model to a coaxial borehole heat exchanger system. Geoenergy Science and Engineering. 227, 211815. DOI: https://doi.org/10.1016/j.geoen.2023.211815

[18] Mahmoodpour, S., Singh, M., Turan, A., et al., 2022. Simulations and global sensitivity analysis of the thermo-hydraulic-mechanical processes in a fractured geothermal reservoir. Energy. 247, 123511. DOI: https://doi.org/10.1016/j.energy.2022.123511

[19] Wang, D., Dong, Y., Li, Y., et al., 2022. Numerical simulation of heat recovery potential of hot dry rock under alternate temperature loading. Unconventional Resources. 2, 170–182. DOI: https://doi.org/10.1016/j.uncres.2022.09.006

[20] Vinsome, P.K.W., Shook, G.M., 1993. Multi-purpose simulation. Journal of Petroleum Science and Engineering. 9(1), 29–38. DOI: https://doi.org/10.1016/0920-4105(93)90026-B

[21] Sanyal, S.K., Butler, S.J., Swenson, D., et al., 2000. Review of the state-of-the-art of numerical simulation of enhanced geothermal systems. Proceedings of the World Geothermal Congress 2000; May 28–June 10 2000; Kyushu-Tohoku, Japan. pp. 3853–3858.

[22] Swenson, D., 1997. User's manual GEOCRACK: a coupled fluid flow/heat transfer/rock deformation program for analysis of fluid flow in jointed rock. Mechanical Engineering Department, Kansas State University: Manhattan, KS, USA. pp. 1–18.

[23] Yamamoto, T., Kitano, K., Fujimitsu, Y., et al., 1997. Application of simulation code, GEOTH3D, on the Ogachi HDR site. Proceedings of the 22nd Annual Workshop on Geothermal Reservoir Engineering; 27–29 January 1997; Stanford, CA, USA. pp. 203–212.

[24] Walters, D.A., Settari, A., Kry, P.R., 2002. Coupled geomechanical and reservoir modeling investigation poroelastic effects of cyclic steam stimulation in the cold lake reservoir. SPE Reservoir Evaluation & Engineering. 5(6), 507–516. DOI: https://doi.org/10.2118/80997-PA

[25] Pruess, K., Oldenburg, C., Moridis, G., 1999. TOUGH2 user's guide, version 2. U.S. Department of Energy: Washington, DC, USA. pp. 210.

[26] Jing, Z., Willis-Richards, J., Watanabe, K., et al., 2000. A three-dimensional stochastic rock mechanics model for engineered geothermal systems in fractured crystalline rock. Journal of Geophysical Research. 105(B10), 23663–23679. DOI: https://doi.org/10.1029/2000JB900202

[27] Wang, P., Yotov, I., Wheeler, M., et al., 1997. A new generation EOS compositional reservoir simulator: part I – formulation and discretization. Proceedings of the SPE Reservoir Simulation Symposium; 8–11 June 1997; Dallas, Texas, USA. pp. 1–11. DOI: https://doi.org/10.2118/37979-MS

[28] Minkoff, S.E., Stone, C.M., Bryant, S., et al., 2003. Coupled fluid flow and geomechanical deformation modeling. Journal of Petroleum Science and Engineering. 38(1–2), 37–56. DOI: https://doi.org/10.1016/S0920-4105(03)00021-4

[29] Chan, T., Guvanasen, V., Stanchell, F.W., 2004. Verification and validation of a three-dimensional finite-element code for coupled thermo-hydro-mechanical and salinity (T-H-M-C) modelling in fractured rock masses. Elsevier Geo-Engineering Book Series. 2, 452–456. DOI: https://doi.org/10.1016/S1571-9960(04)80082-X

[30] Zyvoloski, G., 2007. FEHM: a control volume finite element code for simulating subsurface multiphase multi-fluid heat and mass transfer. LA-UR-07-3359. Los Alamos National Laboratory: Los Alamos, NM, USA. pp. 1–47.

[31] Zyvoloski, G.A., Robinson, B.A., Dash, Z.V., et al., 1997. User manual for the FEHMN application. LA-UR-94-3788, Rev. 1. Los Alamos National Laboratory: Los Alamos, NM, USA. pp. 129. Available from: https://ntrl.ntis.gov/NTRL/dashboard/searchResults/titleDetail/DE00014902.xhtml (cited 17 October 2024).

[32] Kipp, K.L., Hsieh, P.A., Charlton, S.R., 2008. Guide to the revised ground-water flow and heat transport simulator: HYDROTHERM – version 3. U.S. Geological Survey: Reston, VA, USA. pp. 178. Available from: https://pubs.usgs.gov/tm/06A25/pdf/TM6-A25.pdf (cited 19 March 2025).

[33] Podgorney, R., Huang, H., Gaston, D., 2010. Massively parallel fully coupled implicit modeling of coupled thermal-hydrological-mechanical processes for enhanced geothermal system reservoirs. Proceedings of the 35th Workshop on Geothermal Reservoir Engineering; 1–3 February 2010; Stanford, CA, USA. pp. 1–14.

[34] COMSOL Multiphysics, 2023. COMSOL Multiphysics Reference Manual, v6.2. COMSOL: Stockholm, Sweden. pp. 2202. Available from: https://doc.comsol.com/6.2/doc/com.comsol.help.comsol/COMSOL_ReferenceManual.pdf (cited 22 Novem-

ber 2024).
[35] Holzbecher, E., 2013. Coupled hydro-mechanical modelling of deep geothermal heat production. Proceedings of the Fifth Biot Conference on Poromechanics; 10–12 July 2013; Vienna, Austria. pp. 1–10. DOI: https://doi.org/10.1061/9780784412992.226
[36] CMG STARS, 2016. STARS User guide, Advanced Processes & Thermal Reservoir Simulator. Computer Modelling Group Ltd: Calgary, Canada. pp. 1531. Available from: https://studylib.net/doc/27634726/stars-user-guide--2- (cited 3 November 2024).
[37] Encalada, J.R., Quichimbo, E.A., Vázquez, R.F., 2019. Assessing the impact of fracture properties and wellbore configuration on the energy extraction from hot dry rock. Proceedings of the XVII ECSMGE-2019 Geotechnical Engineering Foundation of the Future; 1–6 September 2019; Reykjavik, Iceland. pp. 1–8. DOI: https://doi.org/10.32075/17ECSMGE-2019-1013
[38] Böttcher, N., Watanabe, N., Görke, U.-J., et al., 2016. Geoenergy modeling I Geothermal processes in fractured porous media. Springer: Leipzig, Germany. Available from: https://vip.s3.ufz.de/ogs/public/web/Books/Geoenergy-Model-I/Geoenergy%2BModeling%2BI.pdf (cited 22 February 2025).
[39] Pogacnik, J., O'Sullivan, M., O'Sullivan, J., 2015. Linking TOUGH2 and ABAQUS to model permeability enhancement using a damage mechanics approach. Proceedings of the World Geothermal Congress 2015; 19–25 April 2015; Melbourne, Australia. pp. 1–9.
[40] O'Sullivan, M.J., O'Sullivan, J.P., 2016. Reservoir modeling and simulation for geothermal resource characterization and evaluation. In: DiPippo, R. (ed.). Geothermal Power Generation Developments and Innovation. Woodhead Publishing: Cambridge, UK. pp. 165–199. DOI: https://doi.org/10.1016/B978-0-08-100337-4.00007-3
[41] Li, K.-Q., Yin, Z.-Y., 2025. State of the art of coupled thermo-hydro-mechanical-chemical modelling for frozen soils. Archives of Computational Methods in Engineering. 32, 1039–1096. DOI: https://doi.org/10.1007/s11831-024-10164-w
[42] Pritchett, J.W., Garg, S.K., 1995. A modeling study of the Oguni geothermal field, Kyushu, Japan. Proceedings of the International Geothermal Association 1995; 18–31 May 1995; Florence, Italy. pp. 1727–1733.
[43] Environment Agency, 2019. Review of software used by the oil and gas industry to model hydraulic fracturing. Environment Agency: Bristol, UK. pp. 1–29.
[44] Duplyakin, D., Beckers, K., Siler, D.L., et al., 2022. Modeling subsurface performance of a geothermal reservoir using machine learning. Energies. 15(3), 967. DOI: https://doi.org/10.3390/en15030967
[45] Lei, Z., Zhang, Y., Zhang, S., et al., 2020. Electricity generation from a three-horizontal-well enhanced geothermal system in the Qiabuqia geothermal field, China: slickwater fracturing treatments for different reservoir scenarios. Renewable Energy. 145, 65–83. DOI: https://doi.org/10.1016/j.renene.2019.06.024
[46] Held, S., Genter, A., Kohl, T., et al., 2014. Economic evaluation of geothermal reservoir performance through modeling the complexity of the operating EGS in Soultz-sous-Forêts. Geothermics. 51, 270–280. DOI: https://doi.org/10.1016/j.geothermics.2014.01.016
[47] Sircar, A., Solanki, K., Bist, N., et al., 2022. Enhanced geothermal systems – promises and challenges. International Journal of Renewable Energy Development. 11(2), 333–346.
[48] Wang, Y., Zhang, F., Liu, F., 2024. Thermo-hydro-mechanical (THM) coupled simulation of the land subsidence due to aquifer thermal energy storage (ATES) system in soft soil. Journal of Rock Mechanics and Geotechnical Engineering. 16(6), 1952–1966. DOI: https://doi.org/10.1016/j.jrmge.2023.05.019
[49] Keller, J., Rath, V., Bruckmann, J., et al., 2020. SHEMAT-Suite: an open-source code for simulating flow, heat and species transport in porous media. SoftwareX. 12, 100533. DOI: https://doi.org/10.1016/j.softx.2020.100533
[50] Lu, X., Jordan, K.E., Wheeler, M.F., et al., 2022. Bayesian optimization for field-scale geological carbon storage [in Chinese]. Engineering. 18(11), 96–104. DOI: https://doi.org/10.1016/j.eng.2022.06.011
[51] Pandey, S.N., Singh, M., 2020. Artificial neural network to predict the thermal drawdown of enhanced geothermal system. Journal of Energy Resources Technology. 143(1), 010901-1–010901-8. DOI: https://doi.org/10.1115/1.4048067
[52] García, N.C., Albert, B.J.F., 2023. The HYDROTHERM code as a tool for integrating geophysics in geothermal prospecting [in Spanish]. Boletín Geológico Minero. 134(3), 27–40. DOI: https://doi.org/10.21701/bolgeomin/134.3/002
[53] Podgorney, R., Finnila, A., Simmons, S., et al., 2021. A reference thermal-hydrologic-mechanical native state model of the Utah FORGE enhanced geothermal site. Energies. 14(16), 4758. DOI: https://doi.org/10.3390/en14164758
[54] Zhang, Q., Li, H., Liu, Y., et al., 2025. Effect of fracture parameters on the thermal recovery performance of enhanced geothermal system. Energy Sources, Part A: Recovery, Utilization, and Envi-

ronmental Effects. 47(1), 44–60. DOI: https://doi.org/10.1080/15567036.2024.2440604

[55] Xue, Z., Zhang, K., Zhang, C., et al., 2023. Comparative data-driven enhanced geothermal systems forecasting models: a case study of Qiabuqia field in China. Energy. 280, 128255. DOI: https://doi.org/10.1016/j.energy.2023.128255

[56] Cui, X., Ngai, Y.W.L., 2021. A 3D thermo-hydro-mechanical coupling model for enhanced geothermal systems. International Journal of Rock Mechanics and Mining Sciences. 143, 104744. DOI: https://doi.org/10.1016/j.ijrmms.2021.104744